J Therm Anal Calorim (2012) 108:275–282
DOI 10.1007/s10973-011-1645-z

Thermodynamic behavior of lipid nanoparticles upon delivery of Vitamin E derivatives into the skin: in vitro studies

J. F. Fangueiro · A. S. Macedo · S. Jose · M. L. Garcia · S. B. Souto · E. B. Souto

Received: 26 April 2011 / Accepted: 5 May 2011 / Published online: 18 May 2011

Abstract This article reports the thermodynamic changes of lipid nanoparticles (LN) upon delivery of lipophilic vitamin E derivatives to the skin. Skin penetration of α-tocopherol (α-T) and α-tocopherol acetate (α-Ta) into and across porcine ear skin was investigated in vitro using tape-stripping test in modified Franz diffusion cells. Wide angle X-ray scattering (WAXS) and differential scanning calorimetry (DSC) have been used to characterize the polymorphism of the solid matrix of LN before and after in vitro skin penetration assay. Cetyl palmitate LN with a loading capacity of 20% of vitamin E derivatives (with regard to the lipid matrix) have shown the typical β' modification of waxes, with a crystallinity index (%CI) between 30 and 40%. Mean particle size and shelf life stability was assessed by static (laser diffractometry, LD) and dynamic (photon correlation spectroscopy, PCS) light scattering techniques. Submicron-sized LN were produced, i.e., 99% of LN showed a size below 600 nm immediately after production. A mean size between 180 and 350 nm (polydispersity index < 0.25) was obtained for LN stored at both 8 and 22 °C, and this size range was kept constant for at least 20 days of shelf life. Quantification of α-T and α-Ta in the skin using tape-stripping provided a 3.4-fold increase in the level of actives within the stratum corneum (SC) and 1.3-fold increase in the viable epidermis (VE). LN increased skin penetration of both actives, following a cumulative release during 8 h in modified Franz diffusion cells. The differences in the distribution levels observed between α-T and α-Ta when delivered via LN was due to the different thermodynamic activity of both actives, i.e., following increased partition coefficient of α-Ta into SC and VE, in comparison to α-T.

Keywords Vitamin E · Tocopherol · Vitamin E-acetate · Tocopherol-acetate · Lipid nanoparticles · LN · Porcine ear skin

J. F. Fangueiro · A. S. Macedo · E. B. Souto (✉)
Faculty of Health Sciences, Fernando Pessoa University, Rua Carlos da Maia, 296, Office S.1, P-4200-150 Porto, Portugal
e-mail: eliana@ufp.edu.pt

S. Jose
Department of Pharmaceutical Sciences, Mahatma Gandhi University, Cheruvandoor Campus, 686 631 Ettumanoor, Kerala, India

M. L. Garcia
Department of Physical Chemistry, Faculty of Pharmacy, University of Barcelona, Av. Joan XXIII s/n, 08028 Barcelona, Spain

M. L. Garcia
Institute of Nanoscience and Nanotechnology, University of Barcelona, Av. Joan XXIII s/n, 08028 Barcelona, Spain

S. B. Souto
Department of Endocrinology, Hospital de São João, Alameda Prof. Hernâni Monteiro, 4200-319 Porto, Portugal

E. B. Souto
Institute of Biotechnology and Bioengineering, Centre of Genomics and Biotechnology University of Trás-os-Montes and Alto Douro (CGB-UTAD/IBB), P.O. Box 1013, 5001-801 Vila Real, Portugal

Introduction

The natural form of vitamin E or α-tocopherol is the isomer 2R, 4′R, 8R′-α-tocopherol (RRR-α-tocopherol), known as D-α-tocopherol. The synthetic form has the chemical name of all-racemic-α-tocopherol or DL-α-tocopherol and contains eight stereoisomers [1]. Both the natural and synthetic forms of α-tocopherol (α-T) are reactive oxygen and radical

scavengers, thereby inhibiting lipid peroxidation of cell membranes, minimizing the light- and toxin-induced tissue destruction [2, 3]. For longer shelf life stability, the active is usually obtained as the esters α-tocopherol acetate (α-Ta) or α-tocopherol succinate. These α-tocopherol derivatives have been widely used as cosmetic ingredients in many formulations [2], being their therapeutic effect dependent on the applied concentration and skin penetration degree [4]. Reactive oxygen species are considered one of the major causes of skin aging [5]. Thus, increasingly interest has been raised to the use of natural antioxidants in preventing skin aging and photo-aging in several pharmaceutical and cosmetic formulations. In addition, lipid nanoparticles (LN) have been reported useful as topical drug carriers [6, 7]. Thus, it is most likely that the combination of pure natural low molecular weight antioxidants with LN will provide a synergistic protection against oxidative stress in skin and should be beneficial as a topical photo-protecting system.

Being lipophilic compounds, α-T and α-Ta are suitable candidates for the encapsulation into LN. LN reported here consists of a lipid matrix composed of a blend of lipids (solid and liquid lipids) that melts at temperatures higher than 40 °C [7–9]. The advantage of these carriers is related to the natural source of the raw materials used for their production (biodegradable and physiological lipids and surfactants) [10, 11], highly suitable for topical applications [8, 12]. In addition, scale-up production lines are also well established [13]. Due to their rigid lipid matrix, LN are expected to be stable against coalescence, when produced as aqueous dispersions. Moreover, the matrix should reduce the mobility of encapsulated actives and thus preventing leakage from the matrix during shelf life. Furthermore, since they are composed of biodegradable materials, these systems can be prepared without organic solvents or other toxic additives minimizing the toxicological risk [8].

The interest behind encapsulating antioxidants (α-T or α-Ta) in LN is also related to the occlusive effect of these particles explained by the formation of a highly packed film onto the skin [14–16]. This film improves skin hydration on the application site and consequently enhances skin permeation. The uppermost layer of the epidermis—the stratum corneum—protects the human body against the loss of physiologically important components and against potentially damaging environmental injuries. This layer consists of corneocytes embedded in a lipid enrich matrix [17]. As the lipid-enriched intercellular regions in the stratum corneum are the only continuous domains through this layer, these lipid regions define the pathway along which the lipophilic actives can diffuse across the stratum corneum, and play a prominent role in skin barrier function. In the intercellular spaces dominate different types of lipid molecules, such as ceramides, cholesterol, and free fatty acids.

The purpose of this study was to prepare LN encapsulating α-tocopherol (α-T) or α-tocopherol acetate (α-Ta) inside a solid core composed of cetyl palmitate, and stabilized by a non-ionic surfactant for deeper skin penetration. This article aims at evaluating the polymorphism and crystallinity of LN, of submicron-meter and narrow size distribution, before and after release of α-T and α-Ta onto and through the skin, to ultimately correlate the thermodynamic behavior of lipid matrices with the drug release and penetration profile.

Materials

The actives, α-tocopherol (α-T) and α-tocopherol acetate (α-Ta), were purchased from Sigma-Aldrich Química, S.A. (Sintra, Portugal). The wax cetyl palmitate (CP) and the surfactant Tego Care®450 (polyglycerol-methylglucose distearate) were obtained as gifts from Gattefossé SAS (St. Priest, France). Miglyol®812 (MG, medium chain triglycerides C_8–C_{10}) was provided by Caelo GmbH (Hilden, Germany). Ultrapure water (Milli-Q Plus, Millipore) was home supplied and used throughout.

Methods

Preparation of LN

Lipid nanoparticles were prepared as described elsewhere [18], having 20% of lipid phase ($12\%_{CP} + 4\%_{MG} + 4\%_{\alpha T/\alpha Ta}$) with respect to the total formulation. This lipid phase was melted at 5 °C above the melting point of the solid lipid (56 °C). Simultaneously, an aqueous surfactant solution composed of 1.8% (w/v) of Tego Care®450 was prepared and heated at the same temperature (~60 °C). A pre-emulsion was further obtained by dispersing the hot lipid phase in the hot surfactant solution at 8000 rpm for 1 min, using an Ultra-Turrax T25 (Janke & Kunkel GmbH, Staufen, Germany). The pre-emulsion was homogenized at 60 °C, applying 700 bar and 3 cycles using the pre-heated Avestin Emulsiflex C3 homogenizer (Avestin, Inc., Canada). The obtained product was filled in 50-mL sterile polypropylene centrifuge tubes being immediately sealed. A thermostated water bath adjusted to 22 °C was used as cooling system to control the rate of cooling of the obtained dispersions. Samples were stored at two different temperatures (8 and 22 °C) and their physicochemical stability was monitored for 20 days. Previously to particle preparation, the solubility of the active ingredients in melted cetyl palmitate was determined visually and microscopically.

Polymorphism and re-crystallization analysis

Polymorphism of lipid matrix was assessed by differential scanning calorimetry (DSC) and by wide angle X-ray diffraction (WAXD). DSC analysis was performed using a Mettler Toledo DSC 823e System (Mettler Toledo, Spain) System. Approximately, 1–2 mg of bulk lipid, or equivalent LN dispersion containing similar amount of lipid, were filled into 40 µL aluminium pans and mechanically sealed. DSC analysis was performed at the scan rate of 5 °C/min in the temperature range of 25–85 °C and cooling down to 25 °C. An empty pan was used as a reference. Indium (purity ≥ 99.95%; Fluka, Switzerland) was employed to check the calibration of the calorimetric system. Data were evaluated from the peak areas using the Mettler STARe V 9.01 DB software (Metler Toledo, Spain). Melting points correspond to the maximum of the heating curve. To compare the crystallinity between LN dispersions, the crystallinity index (%CI), which is defined as the percentage of the lipid matrix that has recrystallized after production and during storage time, was calculated according to the following equation [19]:

$$\%\mathrm{CI} = \frac{\Delta H_{\text{Lipid nanoparticles}}}{\Delta H_{\text{bulk material}} \times \text{Concentration}_{\text{lipid phase}}} \times 100$$

where ΔH is the molar melting enthalpy given by J g^{-1} and the concentration is given by the percentage of lipid phase. WAXD analysis (2(= 4–40°) was performed on a PANalytical X′Pert PRO power diffractometer (Almelo, The Netherlands) with copper anode (Cu-Kα radiation, $\lambda = 1.5418$ nm) and X′Celerator detector. The diffractograms were measured at angles $2\theta = 4$–40° with step of 0.017° and count time of 50 s. Prior to analysis, LN dispersions were transformed into a paste using locust bean gum as thickening agent, i.e., 1 mL of dispersion was mixed with ~1 mg of gum and then mounted on a thin glass capillary being fastened to a brass pin.

Particle size and zeta potential analysis

The particle size of LN was determined by laser diffractometry (LD) and by dynamic light scattering (DLS). LD was carried out using a Malvern Mastersizer 2000 (Malvern Instruments, UK) yielding the volume distribution of the particles. Mie analysis of the raw data was applied. For the LD analysis the diameters LD50% and LD90% were used, where, e.g., LD90% value indicates that 90% (volume distribution) of the measured particles possess a diameter below the given size**.** DLS, or photon correlation spectroscopy (PCS), is a non-invasive procedure for measuring the mean size of particles below 3–5 µm and the width of particle size distribution expressed as polydispersity index (PI). Mean particle size (z-Ave) and PI were determined in a Zetasizer Nano ZS (Malvern Instruments, Malvern, UK). The samples were diluted with ultra-purified water to weaken opalescence before measuring z-Ave and PI. Zetasizer Nano ZS was also used to analyze the electrophoretic mobility to determine the zeta potential (ZP) of particles in aqueous dispersion. ZP of LN was also measured in purified water adjusting conductivity (50 µS/cm) with sodium chloride solution (0.9% w/v). The ZP was calculated from the electrophoretic mobility using the Helmholtz–Smoluchowski equation [20]. The processing was run by the software included within the system. Values reported are the mean ± SD of at least three different batches of each LN formulation.

Assay of active ingredients

Accurately weighted amount of 100 mg of α-T or α-Ta was transferred to 100 ml volumetric flask and diluted with ethanol up to the mark. The UV spectra of both actives in ethanol were recorded and a max. 285 nm was observed for both actives, thus all measurements were carried out at this wavelength. A volume of 1.0 ml of each active loaded LN was centrifuged at 5500 rpm for 70 min to separate the lipid and aqueous phases. A volume of 300 µL of supernatant was then diluted with ethanol to 3.0 ml and analyzed by UV spectroscopy at 285 nm using a Helios Gamma spectrophotometer, against a calibration curve obtained in the range of 0.1 to 0.5 mg/ml obeying the Beer's Lambert law. Encapsulation efficiency (%EE) was determined as follows:

$$\%\mathrm{EE} = \frac{\mathrm{Wa} - \mathrm{Ws}}{\mathrm{Wa}} \times 100\ (\%\mathrm{wt})$$

where Wa stands for the mass of α-T or α-Ta added to the formulation and Ws is the mass of active determined in supernatant after separation of the lipid and aqueous phases [21]. For checking the reliability of the present method, pure ethanolic solutions of both actives were also analyzed for accuracy.

In vitro permeation studies

Skin permeation of vitamin E derivatives was assessed in vitro using open (not occlusive) modified Franz diffusion cells mounted with porcine ear skin. Briefly, full thickness skin was mounted on a 28 cm^2 of Franz diffusion cells (10 mg/cm^2), with the dermal side facing downward into the receptor medium (solution of Miglyol®812:ethanol 96% (1:9) (v/v)). To achieve higher reproducibility, the skin slices were allowed pre-hydration with receptor fluid for 2 h before applications of the LN formulations. The donor compartment was filled with 300 mg of each LN formulation. The system was maintained at 32.0 ± 0.1 °C,

and the receptor medium was stirred at 300 rpm for 8 h. Volumes of 100 µL samples were taken after 1, 2, 4 and 8 h and diluted with 900 µL fresh receptor medium. A solution of Miglyol 812:ethanol 96% (1:9) (v/v) served as reference. After each sampling, Franz cells were filled up with receptor medium. At the end of the assay, the absorbance of actives that permeated across the skin was analyzed at 285 nm.

Skin uptake studies

After in vitro permeation analysis carried out for 8 h, the skin was removed from the Franz diffusion cell and pinned to a piece of parafilm with the stratum corneum (SC) facing upward. Excess of non-absorbed active was eliminated by thoroughly washing the skin surface for DSC and WAXS analysis. The skin area that had been exposed to the formulation was tape-stripped 20 times using 3 M Scotch Book Tape 845 (3 M, St Paul, MN, USA). These tape strips were subsequently immersed in a vial containing 10 mL acetonitrile for 24 h, to allow permeant extraction. Extract aliquots were then analyzed by UV at 285 nm. SC removal was almost complete after 15 successive tape-stripping, as indicated by the glistening of the exposed surface, i.e., viable epidermis (VE). The remaining skin VE was cut into small pieces, vortex-mixed for 3 min in 5 mL acetonitrile, and bath-sonicated for 30 min. An aliquot of the filtered homogenate was then analyzed by UV at 285 nm. Removed SC or VE containing complexes were also submitted to the extraction procedure and used as blank. Molar concentrations were determined based on a calibration curve. The extraction of actives was done after 8 h of incubation from wipe-off, SC and VE (tape-stripping, 20 strips). All experiments were carried out in triplicate. Results obtained were subjected to statistical analysis using Student's t test. A difference between mean values was considered to be statistically significant when the p value was ≤ 0.05.

Results and discussion

Cetyl palmitate was the selected solid lipid for the production of LN. This wax has the advantage of a better in vitro degradation rate and lack of in vivo toxicity [22], where the actives also revealed solubility properties (data not shown). The encapsulation of active ingredients within the lipid matrix is influenced by the crystal structure of the solid lipid molecules. This structure is commonly determined by WAXD analysis. For a single crystal, the diffracted X-rays consist of a few lines (Fig. 1a). With powder, due to a random distribution of crystals of lipid, the diffraction pattern consists of a series of concentric

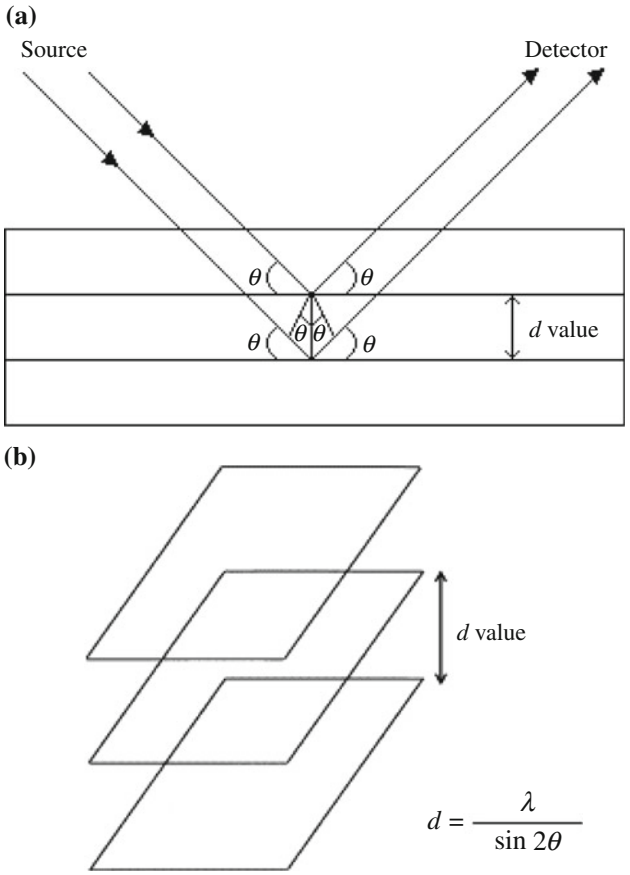

Fig. 1 **a** Schematic representation of X-ray diffraction (modified after Barber [23]) and **b** Cetyl palmitate molecules are arranged in an orthorhombic lamellar lattice structure (modified after [24])

cones with a common apex on the sample. The atoms in a crystal possess the power of diffracting the X-ray beam. Each substance scatters the beam in a particular diffraction pattern, producing a fingerprint for each atom crystal or molecule. If an unknown powder sample is to be identified, its diffraction pattern may be compared with those of known substances or its d values calculated from the diffraction diagram and compared with the d values of known compounds. The interplanar distance d can then be calculated applying the Bragg's equation:

$$d = \frac{\lambda}{\sin 2\theta}$$

In previous studies, it has been observed that cetyl palmitate molecules are arranged in an orthorhombic lamellar lattice structure (Fig. 1b), i.e., the most stable polymorphic form of this lipid is the β' modification. During re-crystallization process, LN usually undergo a polymorphic transition from the metastable α form into the most stable β form. In the present case, a wax (cetyl palmitate) has been used as solid lipid for the production of LN. WAXD patterns of all samples showed two strong

signals, one at 0.42 nm and other at 0.37 nm, which are both characteristic of the orthorhombic perpendicular ($O_{\perp}$) subcell, i.e., β' modification. Thermodynamic stability and lipid packing density increase, while drug incorporation rates decrease from the supercooled melt to α, β', and β modifications [11]. It is therefore most likely that actives such as α-T and α-Ta, will remain entrapped in the lipid matrix during shelf life. For comparison purposes, the crystallization behavior of the dispersed particles was studied by DSC (Table 1).

Within 12 h after LN production, the melting point of the lipid matrix was registered between 42 and 48 °C with heat capacity of $\sim$1 J g^{-1}. The almost constant crystallization temperature observed during 20 days of shelf life at both storage temperatures (8 and 22 °C) indicates a homogeneous nucleation process. The pre-requisite for topical/dermatological administration of LN is the need of an onset value higher than 40 °C, which is the case of both systems (α-T and α-Ta). However, the melting enthalpy was shown to be lower than 10 J g^{-1}, which means a %CI of $\sim$30–40% in all formulations. This is obviously a result of the high loading capacity of LN for the vitamin E derivatives (approx. 20% with regard to the lipid matrix), where the melting point increased from 45.87 to 48.33 °C (in case of $LN_{\alpha\text{-T}}$) and from 45.94 to 49.04 °C (in case of $LN_{\alpha\text{-Ta}}$).

Immediately after production and during the cooling step, the systems were milky dispersions. Furthermore, no gel formation was detected for period of 20 days of shelf life at 8 and at 22 °C. Regarding the physical stability of the aqueous dispersions (Table 2), the mean size of LN remained between 180 and 340 nm for 20 days (with PI < 0.25), showing a narrow size distribution. The high negative electrical charge (>|40| mV) detected at the surface of the carriers contributed to the increase of long term stability of LN. Also LD data emphasized the excellent physical stability of these systems, e.g., 99% of LN < 550 nm after 20 days at both storage temperatures (Fig. 2).

The formulations were placed onto the surface of modified Franz diffusion cells. After 8 h the excess of formulations was wiped off and the amount of actives determined in this excess and in the remaining tissue (at the surface by tape stripping, in the skin, and in the lumen). Figure 3 shows the distribution of α-T and α-Ta from LN formulations in porcine ear skin. The amount of non-penetrated actives was close to 60% for both α-T (58.7%) and α-Ta (56.2%). By tape-stripping, α-T was removed more extensively from the skin surface than its derivative. The affinity of α-Ta to human skin was also emphasized by the amount measured in both SC and VE which was higher than α-T, i.e., the former penetrates better in skin.

Anisotropic diffusion of LN within the pores of the skin was not addressed with this study; therefore, we cannot assume that penetration of LN contributes for the amount of actives measured in the extracts. In addition, the particle size was shown to be similar in both formulations, i.e., 99% below 300 nm on the day of production (Table 2). A possible explanation for these results is solely related to the partition effect of actives within the different layers of the skin.

Depending on their surface characteristics, LN will exhibit different degree of affinity to the skin surface (Fig. 3). As expected, LN with a lipophilic-like surface possess a high degree of similarity with the skin lipids, therefore they might be retained in greater extent onto the application site (Fig. 3A). On the other hand, LN composed of surfactants with a low hydrophilic–lipophilic balance (HLB) value will show a higher tendency to move to surfaces of higher hydrophility (Fig. 3B).

In this work, an amphiphilic surfactant (Tego Care®450) was selected for the production of LN, therefore, the

Table 1 DSC parameters recorded after 20 days of storage at 8/°C and at 22/°C, in comparison to the results obtained on the production day (freshly prepared samples)

Sample	Storage time/days	Storage temperature/°C	Melting point/°C	Onset temperature/°C	ΔT $T_{melting} - T_{onset}$	Integral/mJ	Heat capacity/J g^{-1}
$LN_{\alpha\text{-T}}$	Day 0	Freshly prepared	42.45	40.13	2.32	17.58	0.93
	Day 10	8	42.74	40.61	2.14	99.31	4.61
		22	44.31	41.79	2.52	59.17	2.84
	Day 20	8	42.89	41.04	1.85	180.99	8.24
		22	45.87	42.94	2.93	18.99	1.04
$LN_{\alpha\text{-Ta}}$	Day 0	Freshly prepared	44.34	40.97	3.37	19.15	1.16
	Day 10	8	44.86	41.20	3.67	100.65	4.46
		22	46.43	41.94	4.49	61.82	2.95
	Day 20	8	45.42	41.38	4.04	182.10	7.71
		22	45.94	42.64	3.30	22.96	1.41

Table 2 Mean particle size (z-Ave), polydispersity index (PI), zeta potential (ZP) and volume distribution (d50% and d99%) of LN for 20 days at 8 and 22°C

Formulation storage temperature	z-Ave/nm	PI	ZP/mV	LD/μm d50%	d99%
$LN_{\alpha\text{-T}}$ (freshly prepared)	303.8 ± 2.3	0.094 ± 0.033	−42.3 ± 0.44	0.185 ± 0.013	0.289 ± 0.005
$LN_{\alpha\text{-T}}$ (day 1)					
8/°C	303.7 ± 6.8	0.153 ± 0.082	−40.7 ± 0.4	0.301 ± 0.016	0.562 ± 0.020
22/°C	310.3 ± 8.6	0.132 ± 0.075	−43.4 ± 2.3	0.186 ± 0.001	0.523 ± 0.003
$LN_{\alpha\text{-T}}$ (day 10)					
8/°C	311.9 ± 6.2	0.147 ± 0.057	−47.4 ± 0.5	0.127 ± 0.059	0.530 ± 0.025
22/°C	313.9 ± 2.5	0.123 ± 0.062	−43.7 ± 0.7	0.169 ± 0.013	0.551 ± 0.054
$LN_{\alpha\text{-T}}$ (day 20)					
8/°C	331.3 ± 6.7	0.126 ± 0.069	−47.8 ± 2.2	0.353 ± 0.012	0.521 ± 0.021
22/°C	339.3 ± 6.3	0.129 ± 0.071	−43.7 ± 0.4	0.323 ± 0.033	0.557 ± 0.024
$LN_{\alpha\text{-Ta}}$ (freshly prepared)	184.2 ± 4.3	0.128 ± 0.073	−40.7 ± 0.2	0.134 ± 0.025	0.293 ± 0.034
$LN_{\alpha\text{-Ta}}$ (day 1)					
8/°C	191.2 ± 2.8	0.133 ± 0.065	−40.4 ± 0.8	0.148 ± 0.013	0.436 ± 0.037
22/°C	189.6 ± 2.6	0.215 ± 0.023	−43.3 ± 0.3	0.183 ± 0.002	0.473 ± 0.004
$LN_{\alpha\text{-Ta}}$ (day 10)					
8/°C	309.9 ± 2.3	0.142 ± 0.069	−47.5 ± 1.0	0.150 ± 0.005	0.546 ± 0.002
22/°C	313.9 ± 7.1	0.127 ± 0.057	−46.0 ± 0.1	0.169 ± 0.006	0.549 ± 0.058
$LN_{\alpha\text{-Ta}}$ (day 20)					
8/°C	334.4 ± 4.6	0.133 ± 0.066	−40.4 ± 0.4	0.148 ± 0.010	0.438 ± 0.026
22/°C	331.1 ± 2.7	0.202 ± 0.023	−43.3 ± 0.3	0.183 ± 0.002	0.473 ± 0.003

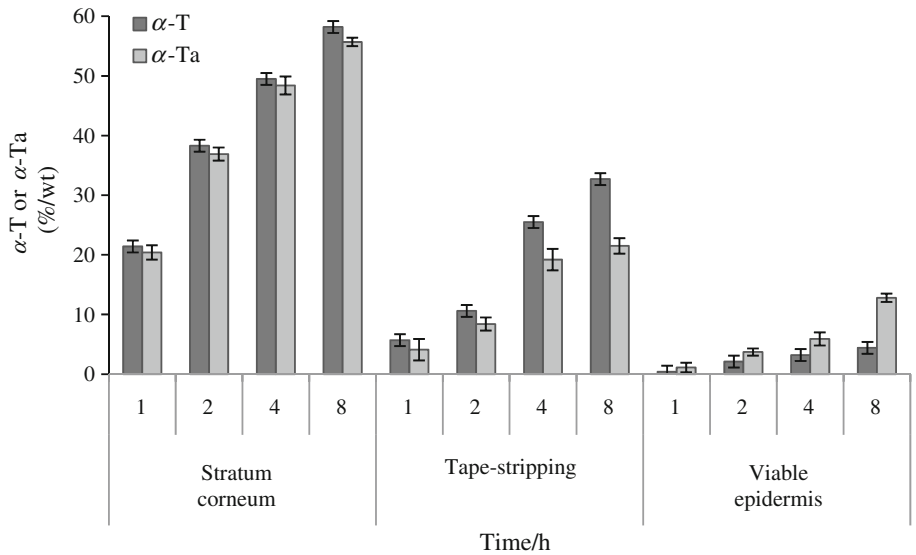

Fig. 2 Partitioning of α-tocopherol derivatives delivered as LN (α-T stands for α-tocopherol and α-T stands for α-tocopherol acetate)

partitioning behavior will be similar in all samples. Tego Care®450 has a HLB value of 12.5, thus in this case, if these particles were placed in an oil/water interface, they would behave similarly to situation C (Fig. 3).

Another point one should consider is the lipid matrix solubility in the skin sebum. LN were analyzed by DSC and WAXS after permeation study. For both $LN_{\alpha\text{-T}}$ (58.7%) and $LN_{\alpha\text{-Ta}}$, the obtained %CI was higher than 40% (data not shown). This means that LN undergo polymorphic changes to expel the loaded actives from the matrix, therefore %CI increases. A well-known property of ultrafine particles is their adhesive behavior when in contact onto surfaces. Particles suffer fusion while transforming from spherical (less crystalline) to platelet-like shape (more crystalline). In

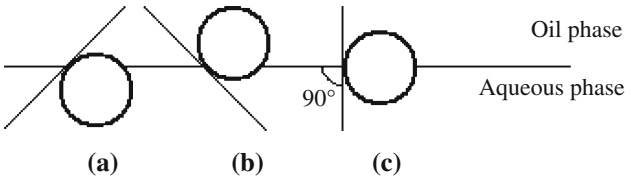

Fig. 3 Partitioning of solid particles at oil/water interfaces according to their surface hydrophilicity. (*A*) hydrophilic-like particles, (*B*) lipophilic-like particles, (*C*) amphiphilic-like particles

addition to the fact that α-tocopherol is an excellent solvent for several poorly soluble [23] and lipophilic drugs [24], these properties together might increase the bioavailability of particular drugs through the topical route. It has also been proposed that polymeric nanoparticles [25] and liposomes [26, 27] are able to penetrate the skin. However, the mechanism used for such attempts still remains under investigation. Despite the biodegradability of LN, in the follicular ducts that mainly contain lipophilic compounds of the sebum, those particles are likely stable. Thus, in order to produce a pharmacological effect the active compound needs to be released from the colloidal carriers by diffusion. Sebum secretion from the pilosebaceous glands usually requires about 8 days [28]. If LN are present, these carriers will be eliminated via sebum secretion after entering the hair follicles, drug release from the nanoparticles has to be much faster than 8 days. Therefore, it is assumed that following topical administration of aqueous LN dispersions, the particles will be specifically located in the pilosebaceous units, being the active released within the lipophilic medium inside the follicular duct. To produce the pharmacological effect, the active will diffuse to its site of action and while empty LN will be eliminated from the follicular duct to the skin surface by the sebum secretion.

Conclusions

Lipid nanoparticles can be considered an approach to deliver lipophilic molecules being solubilized in the oily fraction of LN matrix. If α-tocopherol derivatives can solubilize other pharmacologically active compounds, this may suggest the advantage of combining drugs with these antioxidants in skin designed preparations, both to improve penetration and availability of antioxidants to epidermal layers and to enhance their protective potential. From the obtained results, the real impact of LN on the bioavailability of α-tocopherol derivatives through topical route is difficult to predict, since the actives penetrate differently depending on the tested tissue and on the active itself. However, it can be stated that LN gather relevant features for follicular targeting of active ingredients. Firstly, these particles can reduce the systemic toxicity since a lower active concentration will be required for the pharmacological effect, being also composed of physiological and skin-like lipids. This will contribute to increase the therapeutic index of certain drugs. Moreover, when entrapped into LN transepidermal pathway can be reduced or even avoided, which will enhance the active concentration within the pilocebaceous units.

Acknowledgements The authors wish to acknowledge Fundação para a Ciência e Tecnologia do Ministério da Ciência e Tecnologia, under the reference PTDC/SAU-FAR/113100/2009.

References

1. Burton GW, Ingold KU. Vitamin E as in vitro and in vivo antioxidants. Ann N Y Acad Sci. 1989;570:7–22.
2. Kalka K, Mukhtar H, Turowski-Wanke A, Merk H. Biomelanin antioxidants in cosmetics: assessment based on inhibition of lipid peroxidation. Skin Pharmacol Appl Skin Physiol. 2000;13:143–9.
3. Burgess C. Topical vitamins. J Drugs Dermatol. 2008;7:s2–6.
4. Van Haaften RIM, Evelo CTA, Penders J, Eijnwachter MPF, Haenen GRMM, Bast A. Inhibition of human glutathione S-transferase P1-1 by tocopherol and α-tocopherol derivatives. Biochim Biophys Acta. 2001;1548:23–8.
5. Lam PY, Yan CW, Chiu PY, Leung HY, Ko KM. Schisandrin B protects against solar irradiation-induced oxidative stress in rat skin tissue. Fitoterapia. 2011;82:393–400.
6. Doktorovova S, Souto EB. Nanostructured lipid carrier-based hydrogel formulations for drug delivery: a comprehensive review. Expert Opin Drug Deliv. 2009;6:165–76.
7. Souto EB, Muller RH. Lipid nanoparticles: effect on bioavailability and pharmacokinetic changes. Handb Exp Pharmacol. 2010;197:115–41.
8. Müller RH, Mehnert W, Souto EB. Solid lipid nanoparticles (SLN) and nanostructured lipid carriers (NLC) for dermal delivery. In: Bronaugh L, editor. Percutaneous absorption. New York: Marcel Dekker, Inc.; 2005. p. 719–38.
9. Souto EB, Doktorovova S. Chapter 6—solid lipid nanoparticle formulations pharmacokinetic and biopharmaceutical aspects in drug delivery. Methods Enzymol. 2009;464:105–29.
10. Mehnert W, Mäder K. Solid lipid nanoparticles—production, characterization and applications. Adv Drug Deliv Rev. 2001;47:165–96.
11. Müller RH, Mäder K, Gohla S. Solid lipid nanoparticles (SLN) for controlled drug delivery—a review of the state of art. Eur J Pharm Biopharm. 2000;50:161–77.
12. Müller RH, Radtke M, Wissing SA. Solid lipid nanoparticles (SLN) and nanostructured lipid carriers (NLC) in cosmetic and dermatological preparations. Adv Drug Deliv Rev. 2002;54:S131–55.
13. Dingler A, Gohla S. Production of solid lipid nanoparticles (SLN): scaling up feasibilities. J Microencapsul. 2002;19:11–6.
14. Wissing SA, Lippacher A, Müller RH. Investigations on the occlusive properties of solid lipid nanoparticles (SLN). J Cosmet Sci. 2001;52:313–24.
15. Wissing SA, Müller RH. A novel sunscreen system based on tocopherol acetate incorporated into solid lipid nanoparticles. Int J Cosmet Sci. 2001;23:233–43.
16. Wissing SA, Müller RH. The influence of the crystallinity of lipid nanoparticles on their occlusive properties. Int J Pharm. 2002;242:377–9.

17. Pilgram GSK, van Pelt AME, Bouwstra JA, Koerten HK. Electron diffraction provides new information on human stratum corneum lipid organization studied in relation to depth and temperature. J Investig Dermatol. 1999;113:403–9.
18. Gonzalez-Mira E, Nikolic S, Garcia ML, Egea MA, Souto EB, Calpena AC. Potential use of nanostructured lipid carriers for topical delivery of flurbiprofen. J Pharm Sci. 2011;100:242–51.
19. Freitas C, Müller RH. Correlation between long-term stability of solid lipid nanoparticles (SLN^{TM}) and crystallinity of the lipid phase. Eur J Pharm Biopharm. 1999;47:125–32.
20. Egorova EM. The validity of the Smoluchowski equation in electrophoretic studies of lipid membranes. Electrophoresis. 1994;15:1125–31.
21. Martins S, Silva AC, Ferreira DC, Souto EB. Improving oral absorption of Salmon calcitonin by trimyristin lipid nanoparticles. J Biomed Nanotechnol. 2009;5:76–83.
22. Weyhers H. Feste Lipid Nanopartikel (SLN) für die gewebsspezifische Arzneistoffapplikation, Herstellung, Charakterisierung oberflächenmodifizierter Formulierungen. PhD Thesis, Freie Universität Berlin, Berlin; 1995.
23. Nielsen PB, Müllertz A, Norling T, Kristensen HG. The effect of α-tocopherol on the in vitro solubilisation of lipophilic drugs. Int J Pharm. 2001;222:217–24.
24. Souto EB, Müller RH. SLN and NLC for topical delivery of ketoconazole. J Microencapsul. 2005;22:501–10.
25. Alvarez-Roman R, Naik A, Kalia YN, Guy RH, Fessi H. Skin penetration and distribution of polymeric nanoparticles. J Control Release. 2004;99:53–62.
26. Short SM, Paasch BD, Turner JH, Weiner N, Daugherty AL, Mrsny RJ. Percutaneous absorption of biologically-active interferon-gamma in a human skin graft-nude mouse model. Pharm Res. 1996;13:1020–7.
27. Short SM, Rubas W, Paasch BD, Mrsny RJ. Transport of biologically active interferon-gamma across human skin in vitro. Pharm Res. 1995;12:1140–5.
28. Downing DT, Strauss JS. On the mechanism of sebaceous secretion. Arch Dermatol Res. 1982;272:343–9.